ANAMET Report 044
May 2004

Overmoding transmission characteristics of Type-N connector 7mm line between 18 and 26.5 GHz

B Williams

For further information about ANAMET and its activities contact:

Internet: **http://www.npl.co.uk/npl/clubs/anamet/index.html**

E-mail: **anamet@npl.co.uk**

Comments on this report should be sent to :

Mail: ANAMET
Division of Enabling Metrology
National Physical Laboratory
Queens Road
Teddington
Middlesex
TW11 0LW

Fax: 020 8943 6098 (UK)
+ 44 20 8943 6098 (International)

This report has been approved by the ANAMET Steering Committee

Over moding transmission Characteristics of Type-N connector 7mm line between 18 and 26.5 GHz.

NMS Contract GBBK/C/2/31

B.Williams

22 January 2004

Requests for wider use or release must be sought from:

ASAP Calibration Services Ltd
Universal House
Romsey Industrial Estate
Romsey
Hampshire
SO51 0HR

Administration page

Customer Information	
Customer reference number	Project R1.6b
Project title	Over moding transmission Characteristics of Type-N connector 7mm line between 18 and 26.5 GHz.
Customer Organisation	DTI National Measurement System
Customer contact	Alastair Hooley
Contract number	GBBK/C/2/31, Project R1.6b, Work Package 2
Milestone number	
Date due	January 2004

Principal author	
Enter author	B.Williams
Enter author address	info@asap-cal.co.uk

Release Authority	
Name	J.Luff
Post	Facility Manager
Date of issue	26 January 2004

Record of changes

Issue	Date	Detail of Changes

Abstract / Executive Summary

Recently, measuring instruments, specifically 'spectrum Analysers' operating up to 26.5 GHz, have been introduced fitted with the popular type 'N' as the front panel input connector.

The type-N, of course, is a 7mm connector that is normally restricted to frequencies below 18 GHz this is because, as shown in section 2.2, the cut off frequency of the nearest, high order or waveguide mode, in air spaced, 7mm, 50Ω, coaxial line, is 19.4GHz. Thus there is always the fear that signals above this frequency, transmitted in TEM mode, may degenerate into TE_{11} with a resultant apparent loss as viewed by a TEM receiver terminating the line.

Additionally, as the cut off frequency is considerably lower in dielectrics other than air (Appendix A) there is also a danger that bead resonance could cause problems even below the cut off frequency of 19.4 GHz and as low as 14.5 GHz.

Where mentioned, *literature* cites the TE_{11} (or H_{11}) mode as the nearest waveguide mode on coaxial line, with no reference to any others.

To give some perspective, a range of TE and TM modes were, identified evaluated and tabulated. This confirmed the proximity of TE_{11} and possibly, TE_{21} and TE_{31}.

Calculations were based on data derived from textbooks, printed in the late 1940's and early 1950's. These were in the form of 'look up' tables or graphs against inner and outer diameter ratios of the coaxial line. The scales involved were ill conditioned for 50Ω where the ratio is 2.3026, independent of line size.

As a result, a spreadsheet method has been developed that will yield the cut-off frequency, of the mode of interest, for any inner and outer radius.

In support of theory, both the propagation coefficient and the wave impedance for TE_{11}, are reviewed and an expression for Characteristic impedance, for TE_{11} mode, developed. This is in contrast with previous *literature* where Wave impedance has been used as interchangeable with characteristic impedance.

This report maintains that 'characteristic' impedance is dependent on the nature and geometry of the guiding structure whereas 'wave' or 'field' impedance is independent of these restrictions.

A very considerable amount of measurement data was obtained for various 7mm to 3.5mm adapter combinations at frequencies up to and including 26.5 GHz. This data indicated the possible presence of 'bead resonance' both above and below the cut-off frequency of the TE_{11} mode.

Calculations made with a impedance model indicated a similar situation although exact correlation at frequency points was lacking. However, both the measurement and calculated data seemed very sensitive to small changes.

However, in spite of this, the measurement results clearly indicated that the use of a single, short, adapter previously calibrated for insertion loss and reflection coefficient would be the most prudent approach in the practical situation.

List of contents

1 Introduction

Coaxial line systems are normally operated with the energy transmitted in the *Principal* or TEM mode. The frequency range of this mode is infinite, that is to say there is no *lower* cut-off frequency or theoretical upper frequency limit.

However, coaxial line can also support the so called waveguide modes, TE & TM, but only above a certain critical frequency which is dependant on the line dimensions. Thus in order to ensure single mode propagation it is usual to specify an upper frequency limit, for any particular coaxial line size, below which the nearest waveguide mode can not operate.

For many years now, as a matter of convenience, it has been fairly common for instruments to operate just beyond the upper frequency limit of the particular connector system employed. For example signal generators operating up to 20GHz may use the type N connector which is usually specified to only 18GHz.

Recently, however, instrument manufacturers have introduced a range of measuring equipment operating at frequencies well above the usual specified limit for the front panel connectors fitted to those instruments. Specifically, instruments such as spectrum analysers operating to 26.5GHz have been introduced fitted with the popular type N connector already mentioned above! This situation is causing problems for laboratories wishing to calibrate these instruments since traceability only exists up to the usual operating frequency range.

The purpose of this project was to investigate this situation from both a theoretical and practical point of view.

Theoretical studies into higher order modes and bead resonance's have been undertaken in order to gain an understanding of the underlying relationships and overall situation. These are documented in the following paragraphs and appendices.

Additionally, experiments have been designed and conducted in parallel, with the theoretical studies, to confirm the predicted effects and search for any possible unexpected outcome.

2 Theoretical Background.

2.1 Coaxial Line Modes.

The ‘modes’ of a transmission line designate the distribution of the electric and magnetic fields. Specific modes are indicated by symbols such as TEM, TE_{mn}, and TM_{mn}. The symbol TEM indicates that this mode has both electric and magnetic fields transverse to the axis of the line, (direction of propagation), only. TE_{mn} indicates that modes in this classification have only the electric field transverse to the axis of the line. TM_{mn} indicates that modes in this classification have only the magnetic field transverse to the axis of the line.

This is the American system of nomenclature, which labels modes according to the field component that behaves as it did in free space. Thus, modes in which there is no component of electric field in the direction of propagation are called *transverse electric* (TE_{mn}) modes. Similarly, modes with no component of magnetic field in the direction of propagation are termed *transverse-magnetic* (TM_{mn}).

With equal logic, the British and European systems label the modes according to the component that has behaviour different from that of free space; thus modes are called H_{mn} instead of TE_{mn} and E_{mn} instead of TM_{mn}. Free space mode is referred to as *Principal* rather than TEM.

The subscript ‘m’ denotes the number of full wave intensity variations around the circumference, and ‘n’ represents the number of half wave intensity changes radially out from the centre to the wall.

In mathematical terms, ref.[1], ‘m’ refers to the order of the Bessel-Neumann combination and ‘n’ is the nth root of the derivative of that function.

It is worth mentioning that in some textbooks the modes are identified by the notation TE_{nm} or TM_{nm}, i.e. subscripts reversed. This aligns with the convention adopted by Bessel more than a century and a half ago. That is, the mth root of $J_n(v)$ is defined by $J_n(v_{\mathbf{nm}}) = 0$.

However, whichever convention is used, (m,n or n,m), it is only necessary to remember that the first subscript refers to the ‘order’ of the function and can have a value in the series **0,1,2,3…**, whilst the second subscripts refers to the ‘number’ of the root of the derivative and can only have a value in the series **1,2,3…** Thus either convention identifies a given mode with the same numerical subscripts.

All this applies to both coaxial line and circular waveguide. There is no such risk of ambiguity with rectangular waveguide where the scripts ‘m’ and ‘n’ are commonly used in alphabetical order!

Pictorial diagrams of the electric and magnetic field distribution transverse to the axis of the coaxial line are shown in Figure 1 for some TE and TM modes. These modes degenerate to similar modes in circular waveguide, as the diameter of the centre conductor becomes vanishingly small.

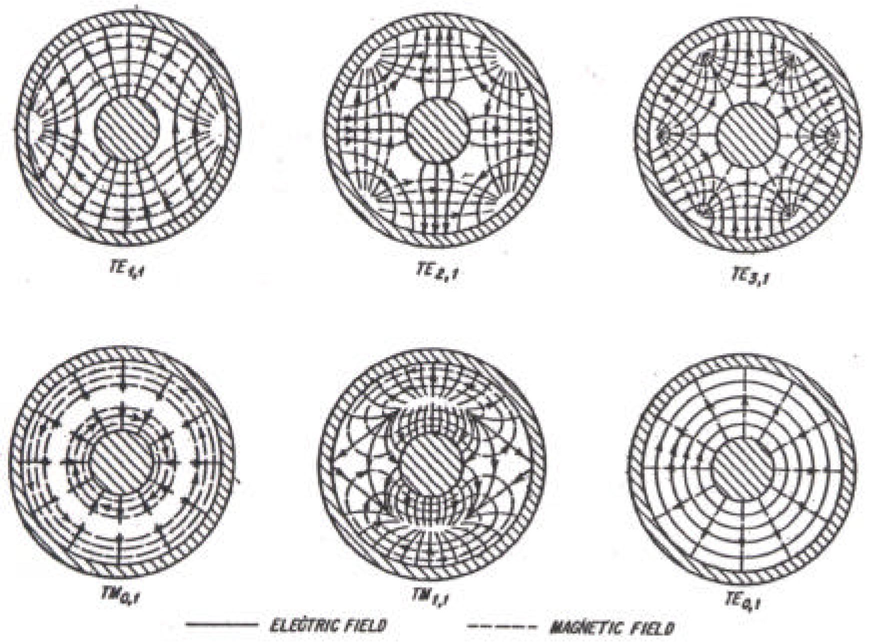

Figure 1 electric and magnetic field distribution transverse to the axis of the coaxial line

The *dominant* mode is the mode with the lowest 'cut off frequency', that is, the frequency below which signal energy is rapidly attenuated and no useful transmission takes place. The dominant mode is *almost* always the only desirable mode, and except for very special applications, an effort is made to *avoid* higher order modes being propagated. TEM is the dominant mode for coaxial line and has no lower cut off frequency.

The first higher-order mode is TE_{11}, (H_{11}). It can be propagated when the frequency is such that one wavelength in the medium between the conductors is approximately equal to the mean circumference of the line. This is as far as most textbooks go on the subject, if indeed it is mentioned at all! They are quite silent on the order of the other modes and how close they may be. Thus, for completeness a range of, TM and TE, modes have been calculated, employing ref.[1], and are listed in Tables 1 and 2.

It is noticeable that the values of cut off frequency for TM modes seem to ascend in a neat pattern whereas the values for TE modes are less well ordered. All the modes, with the exception of TE_{11}, and possibly TE_{21}, even TE_{31} maybe, are well away from the normal operating range of 7mm line. These three are interesting in that their calculation involves the sum of the outer and inner radii of the coaxial line whereas all the other modes are related to the difference of conductor radii.

Mode m,n	Cut-off frequency GHz
TM_{01}	75.1
TM_{11}	77.6
TM_{21}	83.9
TM_{31}	92.3
TM_{02}	151.0
TM_{12}	152.4
TM_{22}	156.6
TM_{32}	163.6
TM_{03}	226.8
TM_{13}	227.8
TM_{23}	231.5
TM_{33}	235.1
TM_{04}	302.6
TM_{14}	303.3
TM_{24}	305.7
TM_{34}	308.9

Table 1 *Higher order modes in 7mm coaxial transmission line*
E-modes or transverse magnetic, $TM_{m,n}$

Mode m,n	Cut-off frequency GHz
TE_{01}	77.6
TE_{11}	**19.39**
TE_{21}	37.98
TE_{31}	55.34
TE_{02}	152.4
TE_{12}	80.7
TE_{22}	85.3
TE_{32}	108.6
TE_{03}	227.8
TE_{13}	153.9
TE_{23}	157.8
TE_{33}	165.5
TE_{04}	303.3
TE_{14}	228.7
TE_{24}	231.8
TE_{34}	237.8

Table 2 *Higher order modes in 7mm coaxial transmission line H-modes or Transverse electric, $TE_{m,n}$*

The values given are as accurate as was possible given that a certain amount of interpolation was necessary. The tables of the roots of the Bessel-Neumann combination (and its derivative) are given in ref.[1] as a function of the ratio of the outer and inner conductor radii. For a 50Ω system this has a value of 2.3026 which necessitated interpolating between 2 and 2.5 in the tables. An alternative source, ref. [2], was used to verify results but also required the same interpolation. This source uses a graphical approach, shown in Figure 2 below. Again, interpolation is necessary, but the plots clearly illustrate the relationship between the various modes in particular showing how TE_{11}, TE_{21} and TE_{31} differ from the others.

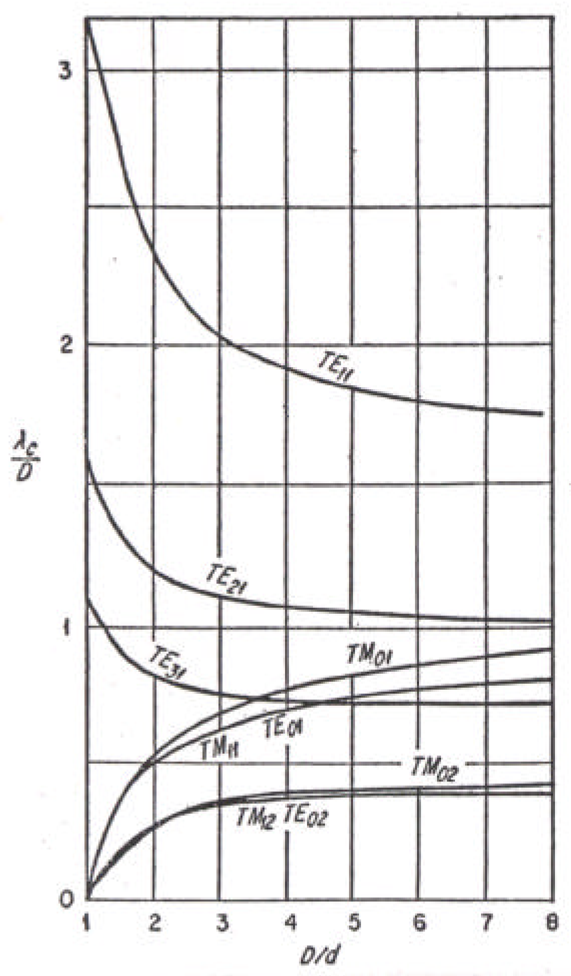

Figure 2 *electric and magnetic field distribution transverse to the axis of the coaxial line*

2.2 Calculation of cut off wavelength of higher order modes in coaxial line.

Having identified that the waveguide mode with the lowest cut off frequency, in coaxial line, is the TE_{11}, the popular formula for the calculation of the cut-off wave length is usually given as:-

$$l_{C^{-}} \cong \frac{p\,(a+b)}{m} \quad \text{for m = 1,2,3.........}$$

Equation 1

For the 7mm line where the internal radius of the tube a = 3.500mm ±0.005mm and the radius of the rod b = 1.520mm ±0.005mm, the cut off wavelength becomes 1.5770795cm.

$$f_c = \frac{v_o}{l_c\sqrt{e_r}}$$

Equation 2

where v_o is the velocity of propagation *in vacuo* 2.99793 10^8 metre/sec and ε_r is the relative permittivity of air, 1.000635 at 20°C, 40% relative humidity. This yields a value of **19.0035 GHz**.

However, the above approximation comes from the more precise formula given in ref.[1]:

$$l_{C^{-}} = \frac{2p}{(c+1)c_{mn}}(a+b) \qquad \text{n = 1 and c = b/a}$$

Equation 3

for c = 2.3026 and m = 1, $(c+1)\chi_{11}$ = 2.0413 and the cut off frequency becomes **19.396 GHz.** A value some 2% higher in this case.

The effect of the ±0.005mm tolerance on both a and b is to vary the cut off frequency by approximately ±20 MHz.

All the above applies to the air spaced section of a coaxial line but, of course, the construction usually includes coaxial beads or spacers to support and align the two conductors. These are normally very short but the relative permittivity of the material involved will be much greater than the 1.000635 of air and will therefore have a considerable effect on the cut off frequency within the beaded section of the line.

For example, if it is assumed that the bead is simply inserted between the two conductors **without** any change in the dimensions of a and b, then the cut off frequency, within the dielectric, can be estimated from Equation 2. A representative value for the relative permittivity might be ε_r = 1.822 (*Teflon, 14mm connectors circa 1965, more modern materials may be lower!*). The resulting cut off frequency would then be **14.369 GHz** within the beaded section of the line.

In reality, inserting the bead in this manner would cause considerable reflections in that region, therefore both the inner and outer conductors are undercut to compensate for the change in relative permittivity and maintain the characteristic impedance at 50Ω.

The above is discussed more fully in Appendix A. Calculations, including the effects of the under cuts, produce a result that is just 0.7% higher at **14.474 GHz.**

Whilst this frequency is well inside the normal operating band for 7mm line it has to be recalled that the bead length is slightly less than 2mm and the cut off wavelength greater than 2 cm ! Further to this, Gilmore ref.[4] discusses the circumstances under which impedance loading may cause the beaded section to resonate within the normal operating frequency of the air spaced line *(this is discussed later in section 4.2).*

2.3 Precise calculation of cut off wavelength of higher order modes in coaxial line.

Both the previous methods, ref.[1 & 2], circa 1950, involve interpolation of either tables or graphs. In both cases the reference scale is the ratio b/a (inner radius of outer conductor / outer radius of inner conductor) which for a 50Ω system will have a value of 2.30263, independent of nominal line size. The scales used in both ref.[1 & 2] are somewhat ill conditioned for this value as will be appreciated from Figure 2.

In 1965, Dimitrios [5] reported a graphical method of calculating TE_{11}, in coaxial line, directly. Returning to first principles the actual line dimensions were used in the transcendental equation:

$$\frac{J'(k_c a)}{N'(k_c a)} = \frac{J'(k_c b)}{N'(k_c b)}$$

Equation 4

where J' is the derivative the Bessel function of the first kind. N' is the derivative of Neumann's function, k_c is the cut-off wave number and a & b are the outer radius of the inner conductor and the inner radius of the outer conductor respectively.

Tables of Bessel functions were used to calculate one side of the equation, which was plotted against k_c. A similar plot for the other side of the equation was obtained by 'proportionality' on the grounds that both limbs are equivalent and that a & b are related by a constant. Intersection of the two plots yields the value of k_c required, which, in turn, allows the cut-off wavelength and frequency to be resolved. Initial plots indicated the region of intersection, which was then plotted on an expanded scale.

Although this method considerably reduced the complexity of the calculations, compared with solving both sides of the equation in a trail and error manner, it was still an enormous task with results being published for 14mm and 7mm air line together with various 7mm cables! *(Note; Dimitrios used a different nomenclature to that used in this report).*

This method lends itself to 'Spreadsheet' application since Bessel functions are available, certainly in Microsoft Excel 97 (*though one needs to appreciate that Neumann function is the same as Bessel function of the second kind, which uses the symbol Y).* With a modern PC it now becomes the work of a few minutes to calculate any cut-off frequencies of interest.

Appendix II gives the detail and extends the general procedure to yield TE_{11}, TE_{12}, TE_{13}, TE_{21} and TE_{31} in particular.

2.4 Transmission lines, Propagation coefficient and Characteristic Impedance

Guiding structures that support TEM waves are usually termed 'transmission lines' to distinguish them from 'waveguide' which can support only TM and TE waves. It follows from this that TM and TE are often referred to as 'waveguide' modes.

The coaxial line, of course, is a 'transmission line' and can support both the principal (TEM) and the waveguide modes.

Knowledge of the Propagation Coefficient and the Characteristic Impedance, of any mode, permits the application of transmission line analysis to predict the impedance and amplitudes at any point on that line.

2.5 Propagation Coefficient

$$g = a + jb$$

Equation 5

is the complex propagation coefficient. Its *real* part α for attenuation due to ohmic and/or dielectric losses or **to the frequency being too low to permit propagation**; its imaginary part β accounts for wave motion.

Practical assumptions are that dielectric materials used in the construction of the line are nonmagnetic ($\mu = \mu_o$) and that the conductors are also nonmagnetic and do not exhibit any dielectric properties such that ($\varepsilon = \varepsilon_o$). Initially it is useful to consider the loss less case in order to present a clear overall view that can be modified to account for small ohmic and dielectric losses later.

For this case of TEM waves on a loss less guiding structure, such as a coaxial line, it follows that:

$$a = 0 \qquad b = v\sqrt{m_o e} = \sqrt{e_r}\, v\sqrt{m_o e_o} = \sqrt{e_r}\,\frac{v}{c} = \frac{2p\sqrt{e_r}}{l}$$

Equation 6

For the case of TM and TE modes, in any guiding structure,

$$g = jk\sqrt{1-\left(\frac{l}{l_{c(m,n)}}\right)^2}$$

Equation 7

where $k = \dfrac{2p\sqrt{e_r}}{l}$

For the above Cut-off case, $\lambda_c > \lambda$ then:

$$g = jb_{TEM}\sqrt{1-\left(\frac{l}{l_{c(m,n)}}\right)^2}$$ *which is pure* Imaginary

Equation 8

For the beyond Cut-off case, $\lambda > \lambda_c$ with a little manipulation it can be shown:

$$g = a = b_{TEM}\sqrt{\left(\frac{l}{l_{c(n,m}}\right)^2 - 1}$$ *which is pure* Real

Equation 9

It may not be immediately obvious but in the above equation α has a limiting value of $\dfrac{2p\sqrt{e_r}}{l_c}$ which for the 7mm line in question translates as 34.6dB/cm (that is 11db/cm at 18GHz and 34.55dB/cm at 1.0GHz).

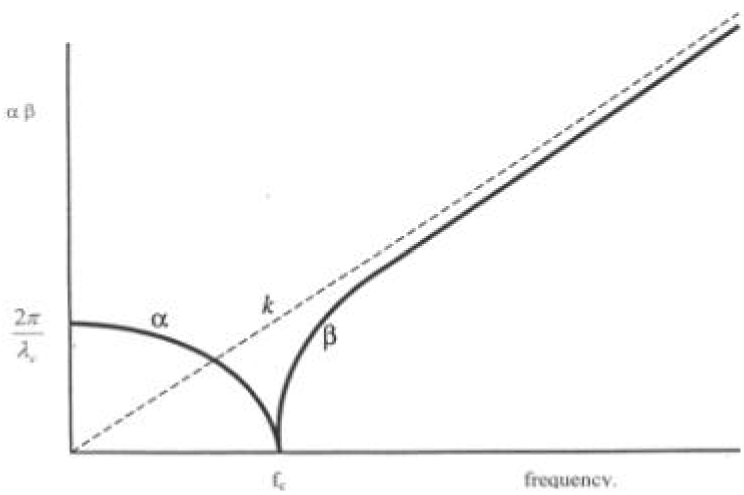

Figure 3 Propagation coefficient g for a coaxial line

The propagation coefficient γ is plotted from Equation 8 and Equation 9 in Figure 3. It illustrates that β approaches 'k' (i.e. β_{TEM}) as the frequency is raised beyond f_c and that α tends towards $2\pi/\lambda_c$ as the frequency decreases below f_c. It will be appreciated that the attenuation described here is not due to losses but rather to the fact that the dimensions of the line are too small to permit propagation in the particular TM or TE mode.

2.5.1 Wave or Field Impedance.

The wave or field impedance is defined as the ratio of transverse components of electric and magnetic fields, $\mathbf{E}_t$ and $\mathbf{H}_t$, which have dimensions of volts/metre and amperes/metre, respectively, thus yielding 'impedance'.

$$Z = \mathbf{E}_t / \mathbf{H}_t$$

Equation 10

This ratio is constant over the guide cross section for any waveguide mode.

For the TEM mode propagating in air (*assumed loss less)* this ratio becomes the well-known 'impedance of free space':

$$Z_{TEM} = \frac{v\, m_o}{g} = \frac{v\, m_o}{v\,\sqrt{m_o e}} = \frac{h}{\sqrt{e_r}} = 376.73\Omega$$

Equation 11

where: γ is the propagation coefficient for the TEM mode, μ_o is permeability of free space, $\varepsilon = \varepsilon_o\varepsilon_r$ where ε_o is the permittivity of free space and ε_r is the relative permittivity which in the case of air is 1.000635 at 20° C, 40% relative humidity and 1013bar atmospheric pressure. $\eta = \sqrt{m_o / e_o}$ is the impedance of free space.

In some textbooks this last term is sometimes referred to as 'Intrinsic Impedance' and given the symbol ζ (zeta). For a little confusion η (eta) is then used as the reciprocal, 'intrinsic admittance'!

For the TE mode the wave impedance becomes as follows below (*i.e. the transverse components ratio together with the substitution of the appropriate propagation coefficient from Eq 6).*

$$Z_{TE} = j\frac{v\, m_o}{g} = \frac{h}{\sqrt{e_r}}\frac{1}{\sqrt{1-\left(\frac{l}{l_c}\right)^2}} \quad for\ l \le l_c \quad or \quad j\frac{h}{\sqrt{e_r}}\frac{1}{\sqrt{\left(\frac{l}{l_c}\right)^2 - 1}} \quad for\ l \ge l_c$$

Equation 12

where λ_c is the cut off wavelength.

For completeness the TM mode wave impedance is given below in a similar manner.

$$Z_{TM} = \frac{g}{jve} = \frac{h}{\sqrt{e_r}}\sqrt{1-\left(\frac{l}{l_c}\right)^2} \quad for\ l \le l_c \quad or \quad -j\frac{h}{\sqrt{e_r}}\sqrt{\left(\frac{l}{l_c}\right)^2-1} \quad for\ l \ge l_c$$

Equation 13

Note. It will be appreciated that there are as many ways, as there are textbooks on the subject, of presenting the foregoing equations, particularly the terms inside the square root. For simplicity of calculation, and symmetry, this report has organised the equations around the l / l_c *ratio.*

2.5.2 Characteristic Impedance

There are several ways of defining characteristic impedance, which depend on the approach to transmission analysis, i.e. 'equivalent distributed circuit element model' or 'wave theory'. Ref.[6] gives a generalised and very useful version based on wave theory.

Briefly this states that the transverse electric and magnetic fields for **any mode** propagating in the positive direction *z* along any rectilinear guiding structure, can be expressed in the form:

$$\mathbf{E}_t(u,v,z,t) = K\mathbf{e}(u,v)e^{j\omega t - \gamma z}$$

$$\mathbf{H}_t(u,v,z,t) = K\mathbf{h}(u,v)e^{j\omega t - \gamma z}$$

With K an amplitude constant and *u,v* transverse co-ordinates.

For a TEM mode it is possible to define a mode voltage V(*z,t*) and a mode current I(*z,t*), as companions to $\mathbf{E}_t$ and $\mathbf{H}_t$, respectively, by employing the integral forms of Maxwell's curl equations.

This eventually leads to:

$$Z_0 = \frac{V(z,t)}{I(z,t)} = -\frac{\int_{P1}^{P2} e.\,dl}{\oint_C h.\,dl}$$

Equation 14

where, in a 2 conductor guiding structure, P1 is a point chosen on one conductor, P2 on the other and C is a contour enclosing one of the conductors.

When equation 14 is applied to the parallel plate guide (TEM mode) it results in the well-known expression:

$$Z_0 = \frac{h}{\sqrt{e_r}} \frac{b}{w}$$ *Equation 15*

Where w is the width of the plates and b is the separation.

A similar result can be obtained, from Equation 14, for stripline (*with idealised field distribution*) namely,

$$Z_0 = \frac{h}{\sqrt{e_r}} \frac{b}{4w}$$ *Equation 16*

and, of course, for coaxial line, Equation 14 yields:

$$Z_0 = \frac{h}{\sqrt{e_r}} \frac{\ln\left(\frac{b}{a}\right)}{2p}$$ *Equation 17*

That is to say, that in each case, the characteristic impedance is the wave (*field, intrinsic or free space*) impedance, $\mathbf{Z_{TEM}}$, of the TEM mode, **times a multiplier which is a function of the geometry of the guiding structure.**

All this is unambiguous and satisfactory for a TEM mode, but difficulties arise when the same concepts of mode voltage and mode current are attempted with the TE and TM modes.

The problem arises because in the TE mode it is **not** possible to define a voltage rise from P1 to P2 that is independent of the path chosen. Similarly for the TM mode it is **not** possible to argue that a closed-contour line integral of $\mathbf{H}_t$ equals the current enclosed.

Generally speaking, there is little need for an actual numerical value, in ohms, which may be quoted as the characteristic impedance of a waveguide. That is to say that the amplitude of Z_0 is usually unimportant since typically impedance *ratios* are used in most applications.

However, there can be occasions when the way in which dimensions enter into the expression for characteristic impedance must be considered. One example would be in predicting the effect of joining two different waveguides.

A more pertinent example, of course, is the subject of this report where two different modes are to be compared on the same guiding structure.

Again, ref.[6] proposes a definition in which the amplitude of the characteristic impedance is arbitrary, due to a free choice of a multiplicative constant but what is important is that the dependency on frequency, dimensions and material parameters is **not** arbitrary.

Two equations are proposed one suitable for TEM and TE modes and a second applicable to TEM and TM modes. Obviously, the first is of particular interest here.

Thus, for TEM and TE modes the characteristic impedance can be evaluated from:

$$Z_0 = \frac{1}{Z_W} \frac{\int_S |e(u,v)|^2 \, dS}{\left[\oint_C h(u,v).\, dl\right]^2}$$

Equation 18

where Z_W is the appropriate wave impedance given in Equation 11 or Equation 12.

Equation 18 is evaluated in Appendix C and yields the not too surprising result that the characteristic impedance for TEM and TE modes on coaxial line is given by:-

TEM

$$Z_0 = \frac{h}{\sqrt{e_r}} \frac{1}{2p} \ln\left(\frac{b}{a}\right)$$

Equation 19

TE

$$Z_0 = \frac{h}{\sqrt{e_r}} \frac{1}{2p} \ln\left(\frac{b}{a}\right) \frac{1}{\sqrt{1-\left(\frac{l}{l_C}\right)^2}} \quad for\ l \le l_C$$

Equation 20

or

$$Z_0 = j\frac{h}{\sqrt{e_r}} \frac{1}{2p} \ln\left(\frac{b}{a}\right) \frac{1}{\sqrt{\left(\frac{l}{l_C}\right)^2 - 1}} \quad for\ l \ge l_C$$

Equation 21

It should be noted that in the 'Waveguide Handbook' ref.[1] and, as a consequence, also in ref.[4], 'Wave Impedance' is christened 'Characteristic Impedance' and employed as such in the usual transmission equations to predict the impedance at a given point on a line.

This results in impedance amplitudes that are approximately 7.5 times greater than the case where Equation 20, above is used.

However, in re-working ref.[4], using both Equation 20 and the original approach, although the impedance magnitudes were quite different the conjugate match frequencies were found to be identical.

On the other hand, when comparing the impedance presented to TEM and TE modes, on the same transmission line, it could be important to have some conformity. For example, for TEM, of course, Z_0 is approximately 50W for all frequencies, whereas, for TE, Z_0 varies from approximately 500W near cut-off to about 200W at much higher frequencies if Equation 20 is used. These numbers become 4000 to 1500W if wave impedance is used as characteristic impedance!

3 The 'Over-mode' Problem

As mentioned in the Introduction, measuring instruments, specifically spectrum analysers operating at frequencies up to 26.5 GHz, have been introduced fitted with the popular type-N as the front panel input connector.

The type-N, of course, is a 7mm connector that is normally restricted to frequencies below 18 GHz. This is because, as shown in section 2.2, the cut off frequency of the nearest waveguide mode, in air spaced, 7mm, 50Ω, coaxial line is 19.4 GHz. Thus there is always the fear that signals above this frequency transmitted in TEM mode may degenerate into TE_{11} mode with a resultant apparent loss as viewed by a TEM receiver terminating the line.

Additionally, as the cut off frequency is considerably lower in dielectrics other than air (Appendix A) there is also a danger that 'bead resonance' could cause problems even below the cut off frequency of 19.4 GHz.

3.1 Practical considerations

Without direct access to any particular instrument the internal configuration cannot be known, but it is a fairly safe assumption that, although, the front panel connector is 7mm the internal transmission lines will be in 3.5mm - more specifically, 3.5mm semi-rigid cable with SMA connectors. This is normal practice, even at very low rf and microwave frequencies, on the grounds of space, cost and convenience.

The simplest situation would then be where a system, operating up to 26.5 GHz in 3.5mm line, is connected to the spectrum analyser via a 3.5mm to type-N male adapter. The analyser input would be type-N female, which in turn may be quickly adapted to 3.5mm (SMA) the other side of the front panel. Thus the majority of the circuit would be in 3.5mm line and at 26.5 GHz well below the cut off frequency of the TE_{11} mode for those dimensions. The problem area will be the short length of 7mm line formed by the two 3.5 to type -N adapters, one belonging to an operator and the other forming part of the instrument. The minimum length of this composite 7mm line is estimated as approximately 7cm.

3.2 Measurement Method

The situation just described can be readily replicated using a suitable Vector Network Analyser (VNA) together with the calibration and verification accessories.

Initially, a full calibration, reflection and transmission, was carried out, on the VNA, from 2 to 26.5 GHz in 3.5mm line. Subsequently, a 3.5mm precision air line, 7.5cm in length was used as a verification artefact in order to highlight any small imperfections in the VNA calibration.

This was considered important since the effects being sort were probably very small, but in this way any 'ripple' (or spikes) present on the verification air line response could be eliminated from the measurement responses of the various adapter combinations under investigation.

All the transmission parameters were monitored, although prime interest was in 'insertion loss' and input reflection coefficient. This data was stored on disc and transferred to Microsoft Excel for convenience of plotting and reproduction.

3.3 Model and calculations.

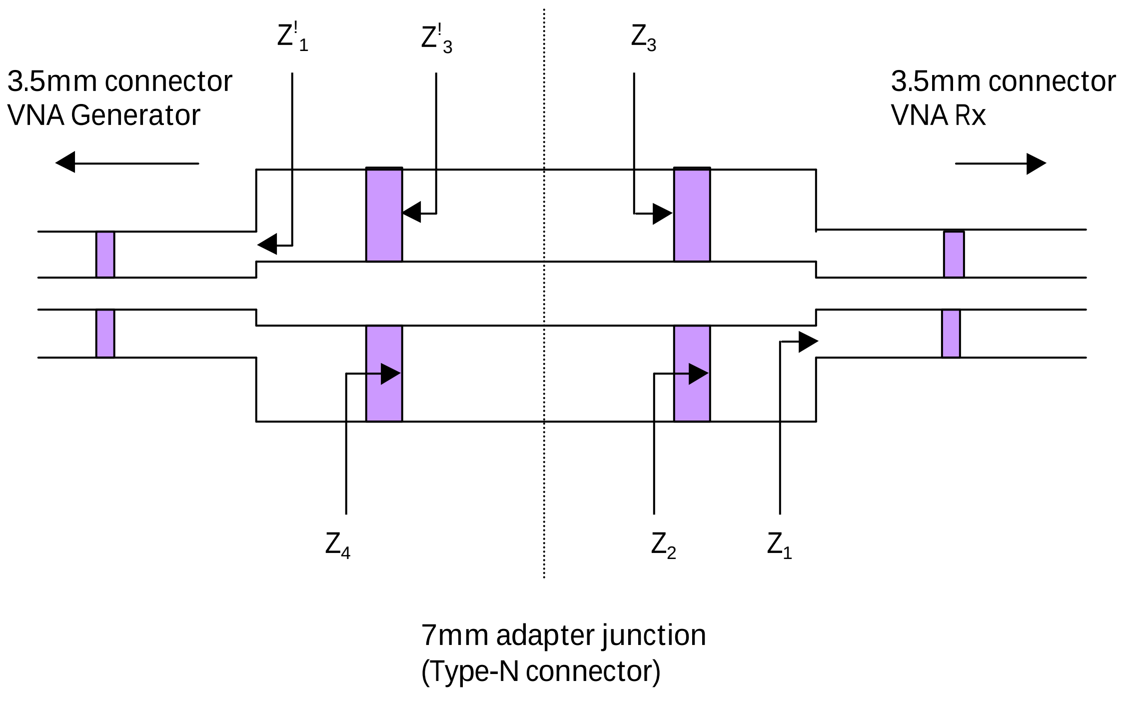

Figure 4 Schematic representation of two type-N adapters mated and inserted at the GPC3.5 connector VNA reference plane of measurement.

Figure 4, above shows a schematic representation of the two type-N adapters mated and inserted at the VNA reference plane of measurement.

The various impedance values, for the TE_{11} mode, of interest are shown. Z_1 is the impedance looking into the 3.5mm line connected to the VNA receiver. Due to the symmetry of the set up Z'_1 will have the same value since this is the impedance looking into the 3.5mm line connected to the VNA generator and both these lines are amplitude and phase matched. The cut off frequency for TE_{11} mode in 3.5mm air line is approximately 38.8 GHz reducing to 28.3 GHz in the dielectric support.

Z_2 is the impedance looking into a length of air spaced 7mm line with Z_1 as a terminating or Load impedance. This was calculated using the general transmission line relationship:

$$Z = Z_0 \frac{Z_L + Z_0 \tanh gl}{Z_0 + Z_L \tanh gl}$$

Equation 22

where :-

Z_L is the load impedance, Z_0 is the characteristic impedance given by Equation 20 or Equation 21, γ is the propagation coefficient given by Equation 8 or Equation 9 and *l* is the length of line between the load and the point of calculation. Most of the components involved here are complex numbers of course.

Obviously Z_3 and Z_4 can be obtained in a similar manner and that Z'_3 will have the same value as Z_3.

It is then of interest to compare Z_3 and Z_4 over the frequency band for any conjugate match points as postulated by Gilmore [4]. These calculations were completed in Microsoft Excel for both below and above cut-off frequencies of the TE_{11} mode.

4 Results and Observations

4.1 Measurement Data

A series of full 2-port measurements were performed on various metrology grade sections fitted with type-N connector line using a Hewlett Packard model 8510C VNA system. The VNA insertable calibration was performed using a GPC3.5 TRL calibration kit between precision test port GPC3.5 connectors. The manufacturer identity of each section remains impartial throughout this report.

The following key has been used for each of the sections:

A = Precision GPC3.5 (M) to N(F) Adapter	Manufacturer A
B = Precision GPC3.5 (F) to N(M) Adapter	Manufacturer A
C = SMA(M) to N(M) Adapter	Manufacturer B
D =SMA(F) to N(F) Adapter	Manufacturer B
E = SMA(M) to N(F) Adapter	Manufacturer C
F = SMA(F) to N(M) Adapter	Manufacturer B
G = N(M) to N(M) Adapter	Manufacturer B
H = N(M) to N(M) Adapter (short air gap)	Manufacturer C
Airline = GPC3.5(M) to GPC3.5(F) 7.5cm unsupported Air Line	Manufacturer A

Figure 5 plots stepped swept insertion loss measurements at increments of 50MHz over a frequency range of 2 to 26.5 GHz.

Figure 5 shows the insertion loss plots of the GPC3.5 connector, 7.5cm long, verification air line. The lower, green, (AB combination), plot represents a laboratory precision pair, literally, gold plated, unsupported GPC 3.5 to precision 'N'. The middle plot, blue, (CD combination), resulted from a 'general metrology standard' adapter pair being SMA to precision type 'N'. All connectors were in very good condition and were 'gauged' in accordance with normal practice.

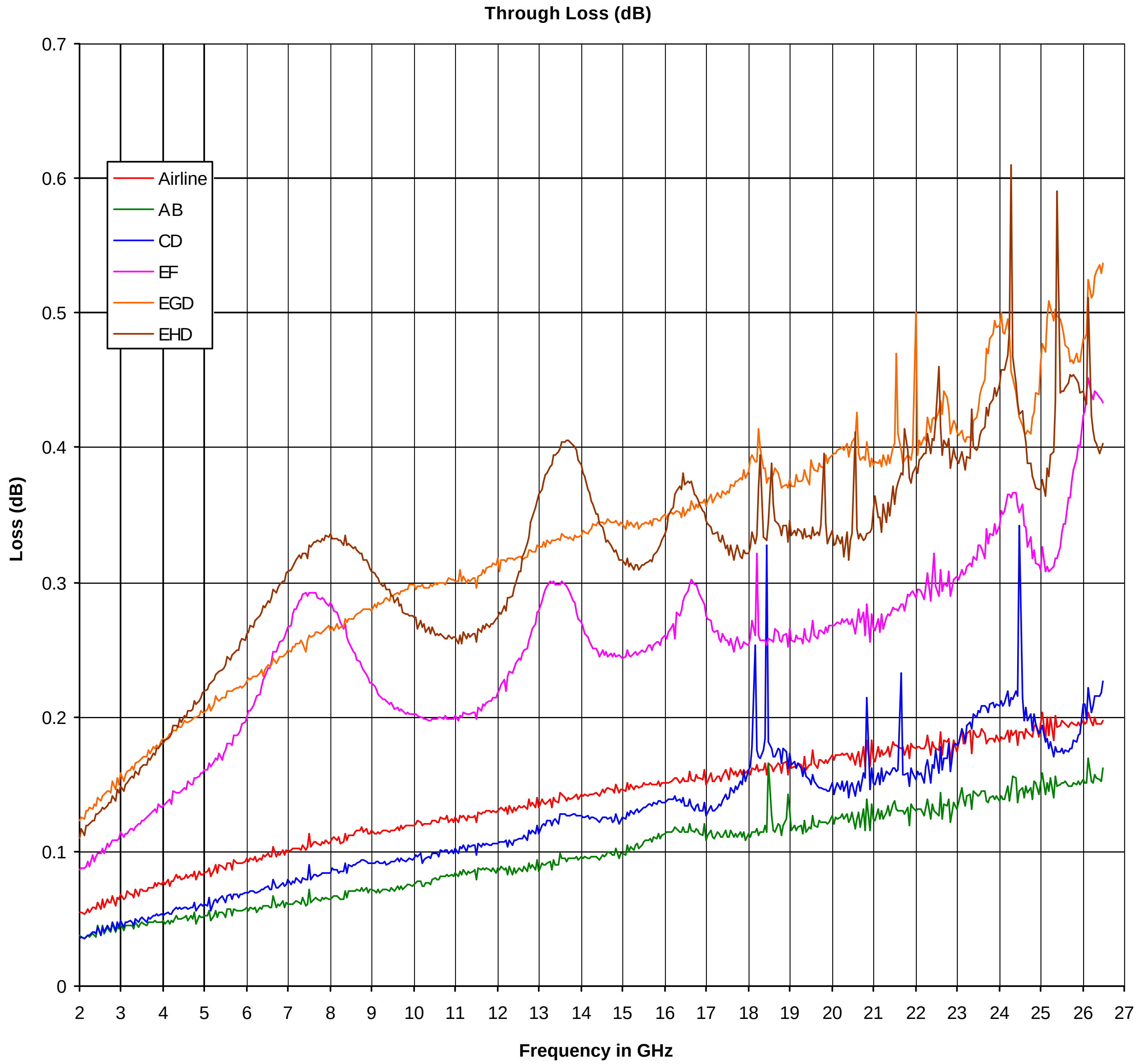

Figure 5 Insertion Loss Comparison

It is interesting to note, that over the majority of the frequency range covered, the insertion loss, of both pairs of adapters, is less than that of the precision verification air line. This of course aligns with theory but any thought that the adapters might be generally superior is quickly dispelled by the reflection coefficient plot, given in Figure 6, where the air line clearly out performs, the best adapter pair, by a considerable margin.

Figure 6 below plots stepped swept reflection coefficient measurements at increments of 50MHz over a frequency range of 2 to 26.5 GHz.

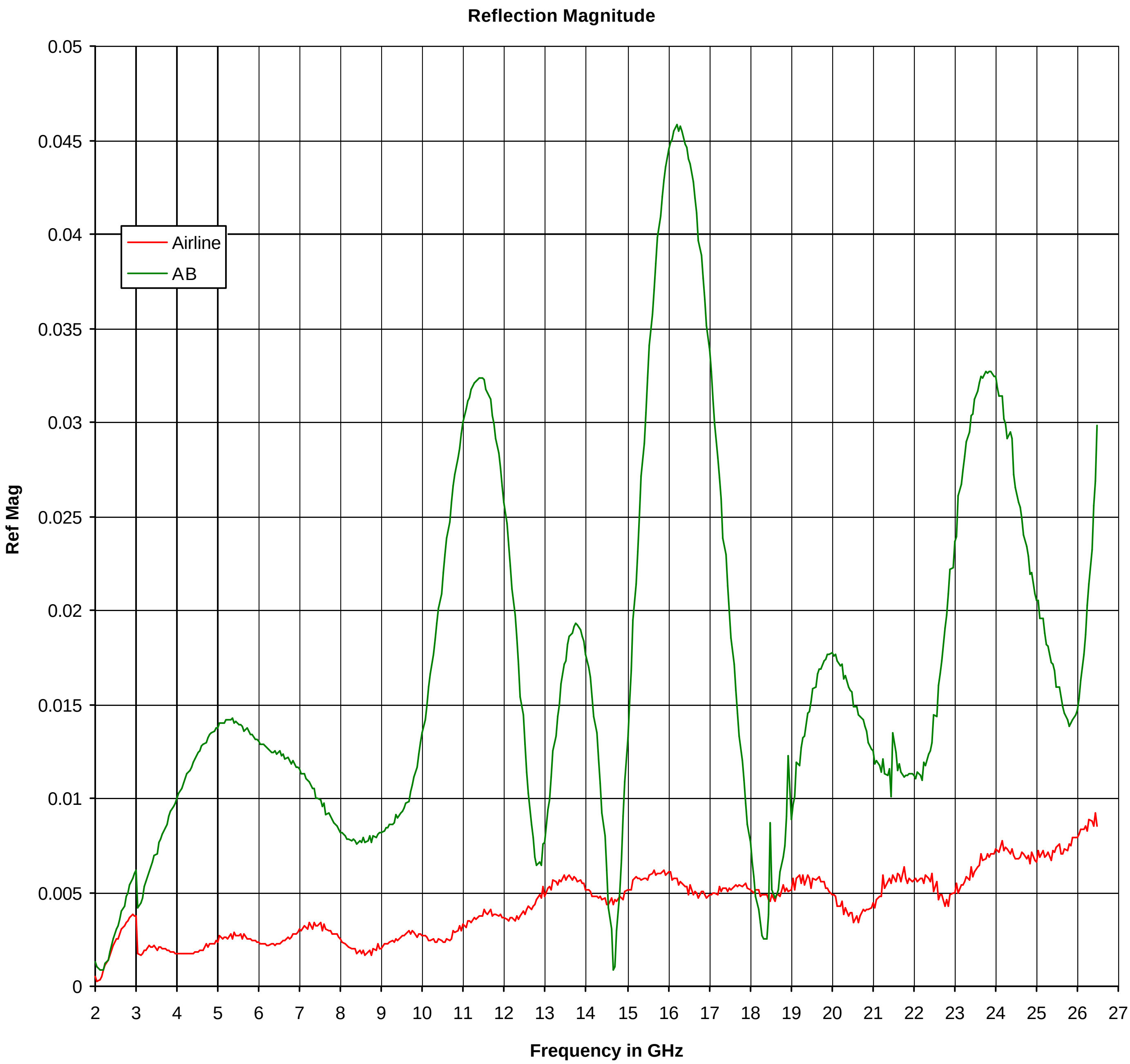

Figure 6 Reflection Coefficient Comparison

Returning to Figure 5, two spikes, possibly representing 'bead resonance', can be seen on both sets of adapter plots between 18 and 19GHz. This is above the normally recommended operating limit of 18 GHz, for 7mm, but below the 19.4 GHz cut off frequency of the nearest wave guide mode TE_{11}.

On the CD, blue plot, there are three further spikes at approximately 20.9, 21,8, and 24.5 GHz. These are not present on the AB, green plot, although inspection of the reflection coefficient response of Figure 6 reveals a small glitch at 21.5 GHz which corresponds to a very small spike on the insertion loss plot, of Figure 5, which is only apparent after careful scrutiny.

In any event, all the spikes are quite small and represent a maximum of 0.05dB on the AB plot and approximately 0.15dB on the CD plot.

Further examples are given in Figure 5, where the adapters discussed above are shown together with two other adapter combinations. Here EF represents a pair of older design, (but not worn out), SMA to type-N, whilst EHD comprises two SMA to type-N female plus a 'back to back', unsupported, male type-N. This last combination shows eight spikes between 19 and 26.6 GHz.

A variety of other adapter combinations, some involving additional lengths of 7mm air line (7.5, 10 and 15cm), were observed with similar results to those shown above.

4.2 Calculated data.

The model discussed in section 3.3 was used to calculate the various impedance values on the transmission line formed by the 7mm adapter pair. In particular the values either side, of a support bead, were compared for conjugate match conditions as this could possibly represent a resonance situation.

This follows from the argument put forward by Gilmore [4]. The bead dielectric will support the TE_{11} above 14.47 GHz but the bead width is less than 2mm whilst the wavelength is in the region of 2cm. However, the argument maintains that the input impedance of the line, to one side of the bead, could at certain frequencies, present a conjugate match to the impedance formed by the bead itself and the other side of the line.

This could encourage the TE_{11} mode, within the bead, but the mode would be unable to propagate outside the bead since the air spaced line is 'below cut –off'. *In the world of dielectric measurement this situation was sometimes referred to as a 'ghost mode' [7] technique where a resonance was deliberately induced in a dielectric sample but at such a frequency that would not allow it to propagate in the air space either side.*

The above was investigated, from 14 to 19.5 GHz, by calculating the impedance either side of a particular bead support. Results are given in Figure 7, below, where the reciprocal of the sum of the impedance, either side of a bead is plotted against frequency.

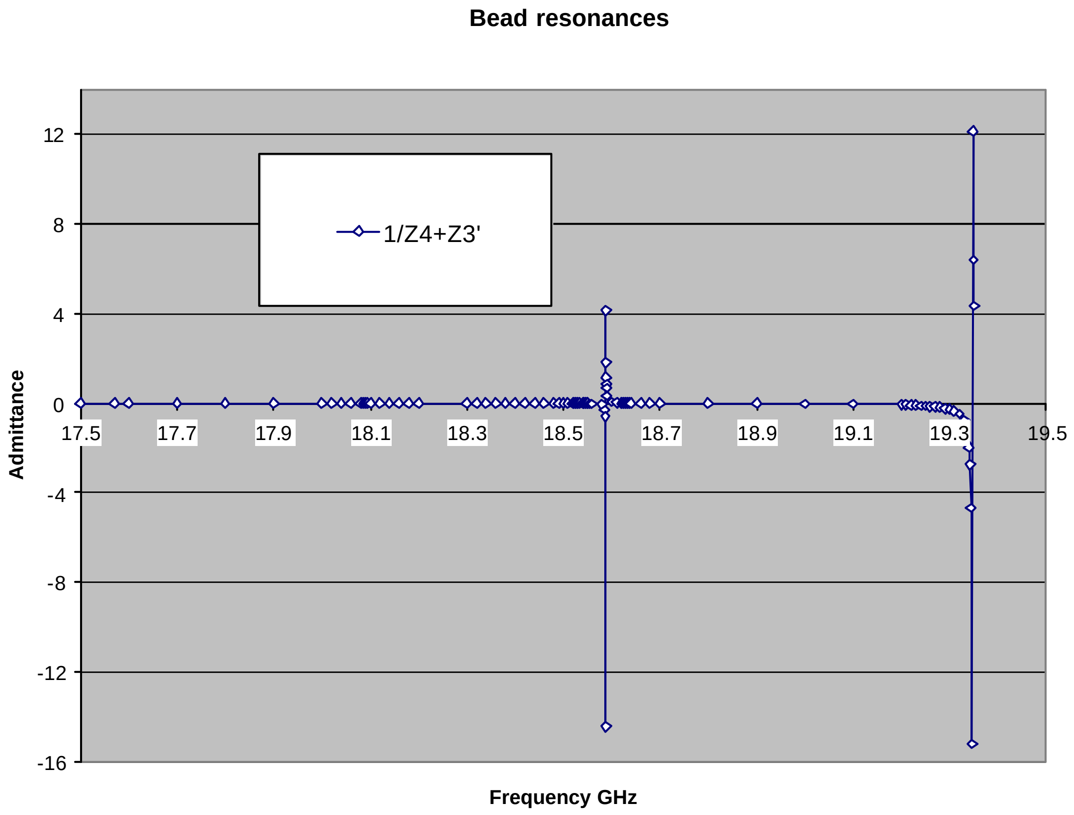

Figure 7 Calculated plot of bead resonance characteristics in a 3mm to 7mm connector adapter pair at frequencies below the cut-off frequency of TE_{11}

This indicates the possibility of resonance within the dielectric support at frequencies of 18.59 GHz and 19.36 GHz. The calculations are sensitive to dimensions, in particular, the width of the bead and the dielectric constant (relative permittivity). No attempt has been made to optimise this data with respect to the measured results.

Above the cut off frequency of TE_{11}:

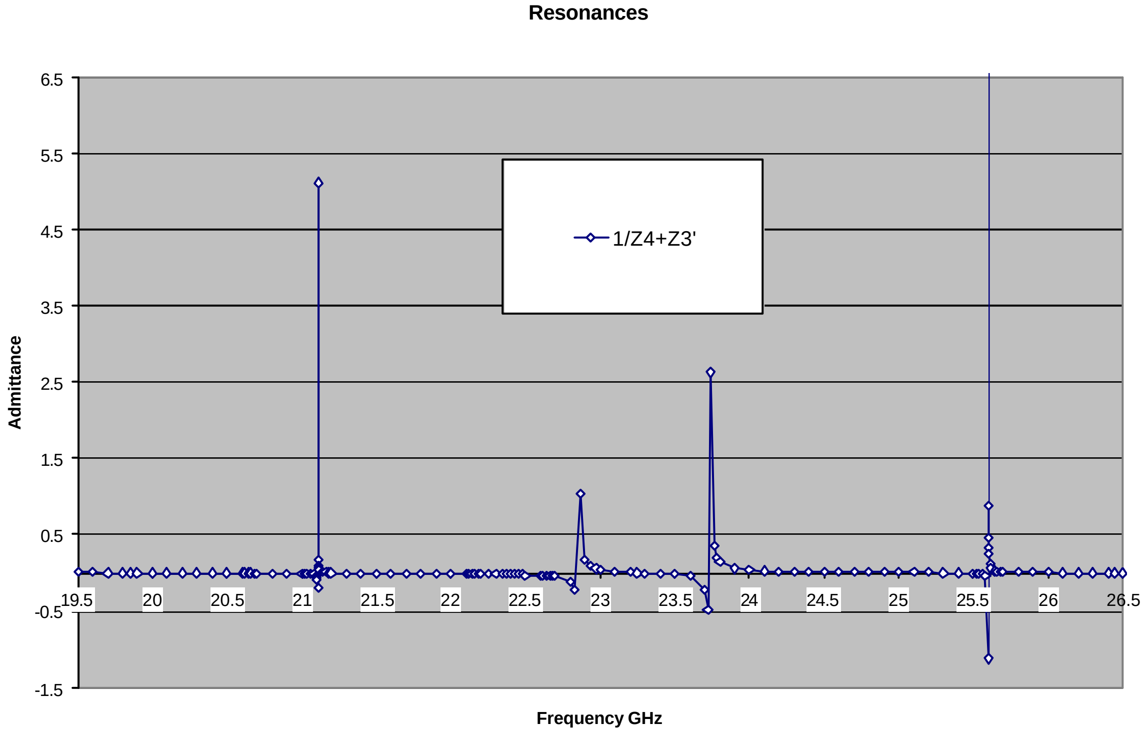

Figure 8 Calculated plot of bead resonance characteristics in a 3mm to 7mm connector adapter pair at frequencies above the cut-off frequency of TE_{11}

Similar calculations for the above cut-off situation are shown in Figure 8 above. Here, again the sharp spikes represent frequencies where conjugate conditions exist at the bead, which could encourage the TE_{11} mode.

5 Conclusions

5.1 Below cut-off

The measured data shows two spikes in both insertion loss and reflection coefficient between 18 and 19.4 GHz, i.e. below cut off.

On the 'AB' adapter these occur at 18.6 and 19 GHz, whereas for the 'CD' adapter the corresponding points are at 18.1 and 18.6 GHz. These two pairs of adapters, as far as can be seen, are very similar in size and construction, but obviously, are not identical!

Calculations from the impedance 'model' also suggest two frequencies where 'bead resonance' may be possible at 18.6 and 19.3 GHz!

Whilst the correlation here is not very good. It must be remembered that the model was found to be sensitive to several parameters, which in turn, were not precisely known. The measurement data also seems to demonstrate a similar sensitivity, in that, the results for two similar pairs of adapters, are quite different but still within the region of the calculated values.

5.2 Above cut-off

Here, again, different adapter sets produced quite different results that only loosely align with the calculated data.

However, the big question here is, *if* the spikes represent the TE_{11} resonating within the bead, *why* does it not continue to propagate and cause more pronounced effects?

Again, although the model suggests similar regions of possible resonance, the correlation is far from precise. However, again the measurement data was sensitive to particular adapter pairs and the 'model' was equally dependant on the same parameters as mentioned in the 'below cut off' case.

5.3 General

It is also worth mentioning that the model takes no account of any possible 'recess' in the inner or outer conductors of the connectors that would produce a discontinuity of the various mating planes. This latter effect may explain the differences between connector pairs.

As a general observation, it would seem worthwhile to re-calculate the model with a more precise knowledge of the dimensions of a particular pair especially the width of the bead and the 'relative permittivity' of the dielectric support.

6 Recommendations

One of the prime objectives was to identify possible problems that might arise when making measurements, above the TE_{11} mode cut off frequency, in 7mm line.

To this end, the data collected, would seem to indicate that, at present, the safest approach would be to keep as much of the system as possible in 3.5mm (*recommended upper limit 26.5 GHz)* and adapt to 7mm via a single short adapter, the mate being on the instrument front panel.

Moreover, it may be an advantage to use a 'laboratory precision' version though these are both costly and fragile at the 3.5mm end due to the absence of a dielectric bead support. High cost issues could be addressed if connectors of such design became commonplace and subsequently manufactured in larger quantities.

A more practical approach would be a ' general metrology' grade adapter **but** one that has been calibrated, on an VNA, for 'insertion loss' and 'reflection coefficient' at frequencies up to 26.5 GHz as described in section 3.2.

7 References / Bibliography

[1] N Marcuvitz. 'Waveguide handbook', section 2.4, IEE Electromagnetic Waves Series 21. 1986.

[2] Moreno. 'Microwave Transmission Design Data', fig 4.7, McGraw-Hill 1948.

[3] J R Whinnery, H W Jamieson, and T E Robbins, ' Coaxial line Discontinuities', Proc. IRE Vol 32, November 1944.

[4] J F Gilmore *'TE_{11} mode resonances in precision coaxial connectors'* General Radio Experimeter, pp 10 – 13, August 1966.

[5] J Dimitrios *'Exact Cut-off Frequencies of Precision Coax'* Microwaves, pp 28 – 31, June 1965.

[6] Elliot S 'An introduction to guided waves and microwave circuits'

[7] G B Walker and S P Luthra 'Use of Ghost Modes to determine Dielectric Constant and Loss Tangent' Proc. IEE Vol 109 Part B supplement No.23, pp 853, September 1961.

[8] S Ramo, J R Whinnery, and T Van Dvzer 'Fields and Waves in Communication Electronics'

[9] E Kreysizig 'Advanced Engineering Mathematics', pp185-186, John Wiley & Sons, 2nd Edition 1967.

Acknowledgements

Thanks go to Steve Harter for the technical editing effort and Peter Constable for numerous adapter measurements on the VNA systems.

A Appendix A Effect of the 'under-cut section' on the cut-off frequency, in the bead area

A.1 Background

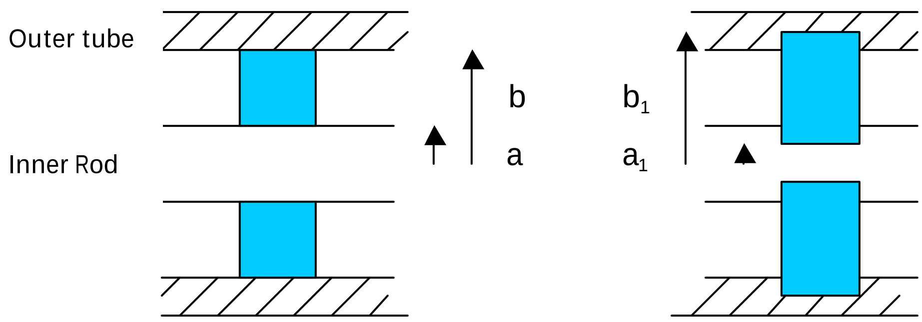

Figure 9 Cross section of coaxial line showing different designs of support bead

Figure 9 above shows a section through a coaxial line where 'b' is the inner radius of the outer tube and 'a' is the radius of the inner rod. The shaded area represents the dielectric support. In the second view both the outer tube and inner rod have been under cut to house a slightly larger dielectric support and the new radii become b_1 and a_1.

A.2 1St Case

The cut off wavelength for The TE_{11} mode in an air spaced coaxial waveguide may be calculated from:

$$l_{C''} = \frac{2p}{(c+1)c_{mn}}(a+b)$$

Equation 23

where 'a' and 'b' are defined in Figure 9, m = 1 & n = 1. χ_{mn} is the *n*th root of the derivative of the Bessel-Neumann combination $Z_m(c\chi_l')$ with c = b/a

For a 7mm 50Ω line with b = 3.5mm and a = 1.52mm, c = 2.3026 and Equation 23 yields $(c+1)\chi_{11}$ = 2.0413.

This in turn leads to a cut off wavelength of 1.545172cm that is equivalent to a frequency of 19.3956GHz.

The cut off frequency in the support is:

$$f_{c_d} = \frac{v}{l_{c''}\sqrt{e_r}}$$

Equation 24

where v is the velocity of propagation in air and e_r is relative permittivity of the support.

In the above case ε_r is estimated as 1.822 resulting in a cut frequency of 14.369GHz.

A.3 2nd Case

The above calculations use the same inner and outer radii, ‘a’ and ‘b’, for both the air spaced and dielectric (support) sections which is not true. In practice both the inner and outer conductors will be under cut for the reasons given below.

The characteristic Impedance, Z_0, can be defined in terms of the distributed parameters of inductance L and capacitance C as:

$$Z_0 = \sqrt{\frac{L}{C}}$$

Equation 25

where:

$$L = \frac{m_0}{2p}\ln\left(\frac{b}{a}\right)$$

Equation 26

and

$$C = \frac{2pe_0e_r}{\ln\left(\frac{b}{a}\right)}$$

Equation 27

$\mu_o = 4\pi/10^7$ Henries per metre $\varepsilon_o = 10^7/4\pi v_o^2$ Farads per metre
$\varepsilon_r = 1.00649$ for air

$v_o = 2.99793 . 10^8$ metres per second. i*n vacuo.*

For the air spaced section considered in the 1st case L will have a value of $1.66811. 10^{-7}$ Henries per metre and C will be $6.67445. 10^{-11}$ Farads per metre, resulting in Z_o = 49.9924Ω.

If the support is now simply inserted in the line as indicated in the first diagram, ε_r will be 1.822, which will almost double the capacitance C to 1.2153. 10^{-10} Farads per metre, and, with L remaining unchanged, the Characteristic Impedance of this support section would become 37.049Ω. This would result in very large reflections at the support.

This increase in capacitance caused by the support can be compensated by under cutting both the inner and outer conductors, by equal amounts, to increase the inductance proportionally. However this is a transcendental situation in that whilst the under cutting *increases L* it will simultaneously *decrease C*!

In the present situation if 'b' is increased to 'b_1 = 3.7905mm' and 'a' decreased to 'a_1 = 1.2295mm', L will become 2.25178 10^{-7} Henries per metre, C will be 9.0028 10^{-11}. This yields characteristic impedance of 50.012Ω.

Returning now to the calculation of cut off wavelength and frequency with these new dimensions, (a+b) will remain unchanged, of course, but the ratio c = b/a will increase from 2.3026 to 3.083!

Figure 10 is a graph of $(c+1)\chi_{11}$ plotted against c taken from the table given in [1]. This indicates that although the change in the value of c represents a significant shift along the x-axis the corresponding change in amplitude is relatively small, being 2.0413 for c = 2.3026 and 2.0562 for c = 3.083 as in this present case.

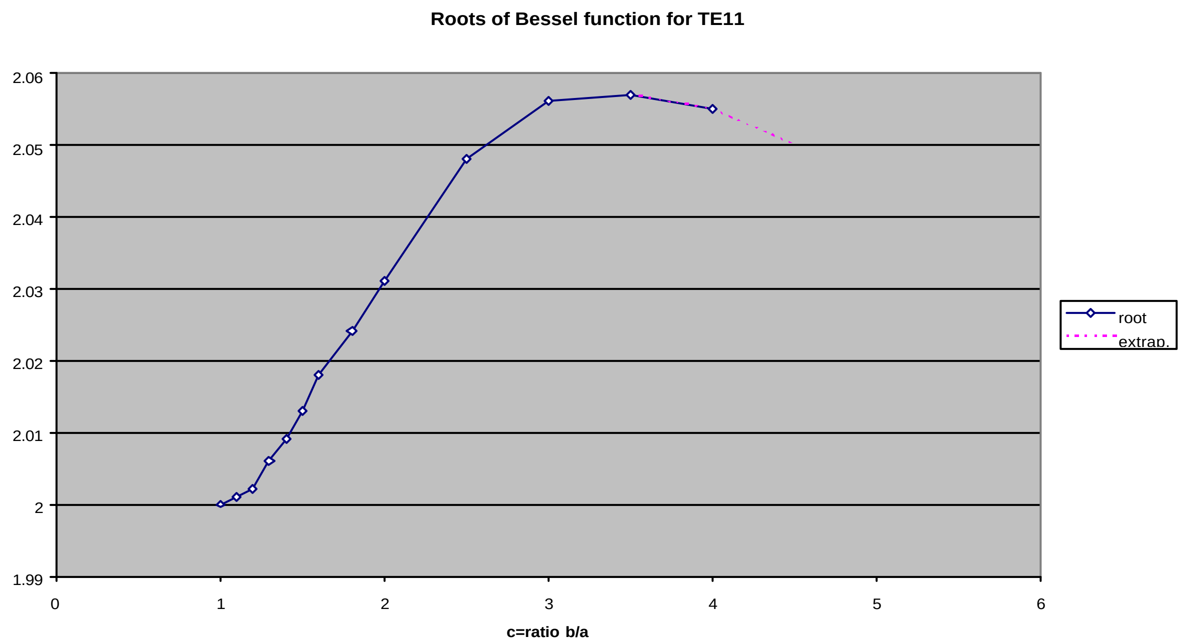

Figure 10 Roots of Bessel Functions for TE_{11}

For values of c larger than 4 it is recommended that [2] be employed where continuous plots from c = 1 to 8 are given.

Completing the calculation for the cut off frequency of the support with the under cut dimensions returns a value of **14.474 GHz.**

Compared to the first calculation of 14.369 GHz, the above value represents an increase of just over **0.7%** which is not wildly significant but has been used in all subsequent calculations for completeness.

The compensation technique, just described, is, in reality, a little more complicated. This is because the under cut itself will cause a small discontinuity capacitance either side of the step in the inner and outer conductors. This may be compensated, by machining a small relief into the front and rear faces of the support bead, as is shown exaggerated, in Figure 11. [3] Describes how to calculate many such discontinuities.

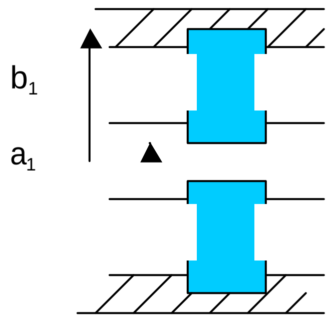

Figure 11 Cross section of coaxial line with machined relief's for support bead

B Precise calculation of the cut-off wavelength, of higher order modes, in coaxial line

B.1 Background

Both the methods, Marcuvitz and Moreno, ref.[1 & 2], circa 1950, involve interpolation of either tables or graphs. In both cases the reference scale is the ratio b/a (inner radius of outer conductor / outer radius of inner conductor) which for a 50Ω system will have a value of 2.30263, independent of nominal line size. The scales used in both ref.[1 & 2] are somewhat ill conditioned for this value as will be appreciated from Figure 2.

In 1965, Dimitrios, ref.[5], reported a graphical method of calculating TE_{11}, in coaxial line, directly. Returning to first principles the actual line dimensions were used in the transcendental equation:

$$\frac{J_1'(k_c a)}{N_1'(k_c a)} = \frac{J_1'(k_c b)}{N_1'(k_c b)}$$

Equation 28

where J' is the derivative the Bessel function of the first kind. N' is the derivative of Neumann's function, k_c is the cut-off wave number and a & b are the outer radius of the inner conductor and the inner radius of the outer conductor respectively.

Tables of Bessel functions were used to calculate one side of the equation, which was plotted against k_c. A similar curve for the other side of the equation was obtained by 'proportionality' on the grounds that both limbs are equivalent and a & b are related by a constant. The intersection of the two curves yields the value of k_c required, which, in turn, allows the cut-off wavelength and frequency to be resolved. Initial plots indicated the region of intersection, which was then plotted on an expanded scale.

Although this method considerably reduced the complexity of the calculations, compared with solving both sides of the equation in a, trail and error, manner, it was still an enormous task with results being published for 14mm and 7mm air line together with various 7mm cables! *(Note; Dimitrios used a different nomenclature to that used in this report).*

This method lends itself to a spreadsheet application since Bessel functions are available, certainly in Excel 97 (*though one needs to appreciate that Neumann function is the same as Bessel function of the second kind which uses the symbol Y).* With a modern PC it now becomes the work of a few minutes to calculate any cut-off frequencies of interest.

B.2 Equations for TE_{11}, TE_{12}, TE_{13}

Equation 28 above is in derivative form but only non-derivative Bessel functions are available in Excel 97 so it is necessary to convert Equation 28 using the 'Recurrence relations', Kreyszig ref.[9].

Dimitrios [5] used a different reference, to the same end, but there are several facets to this theorem, which are needed for the modes beyond TE_{11} which are not considered in [5].

From [8]

$$x^v J_v'(x) = x^v J_{v-1}(x) - v x^{v-1} J_v(x)$$

Equation 29

If $v = 1$ then,

$J_1'(x) = J_0(x) - 1/x J_1(x)$ which applied to B1 yields :

Equation 30

$$\frac{J_0(k_c a) - \frac{1}{k_c a} J_1(k_c a)}{N_0(k_c a) - \frac{1}{k_c a} N_1(k_c a)} = \frac{J_0(k_c b) - \frac{1}{k_c b} J_1(k_c b)}{N_0(k_c b) - \frac{1}{k_c b} N_1(k_c b)}$$

Equation 31

Note k_c has the dimensions of radians/metre and is sometimes referred to as phase constant. The relationship to a and b of the propagation coefficient is illustrated in Figure 3.

Both sides of Equation 29 can be evaluated in a spreadsheet and plotted separately against k_c as shown in Figure 12.

Here '*y*' represents the RHS of the transcendental Equation and '*y*'' the LHS. The cross over point can be seen to be approximately 400 rads/m on the x-axis. It is now a simple matter of 'insert column' and iteratively step the 'x' value until the RHS minus LHS is close to zero (10^{-7} for instance). All of which can be achieved in less time than it takes to describe it here.

A more sophisticated approach would be to do the same thing in 'Visual Basic' where the iterative stepping could be programmed in automatically.

Having determined the value at the intersection, the cut-off wavelength and thence frequency, can be evaluated from :

$$k_c = \frac{2p\sqrt{e_r}}{l_c} \quad \text{and} \quad f_c = \frac{v_0}{l_c\sqrt{e_r}}$$

For the case in point, Figure B1, k_c was determined to be 406.685126 rad/m (difference between RHS and LHS, 6 x 10^{-9}), giving a cut off wavelength of 1.5454697cm and a cut off frequency of 19.39194 GHz. This compares well with

19.39571 GHz obtained from the tables of ref.[1] and the value of 19.3842 GHz quoted in ref.[5].

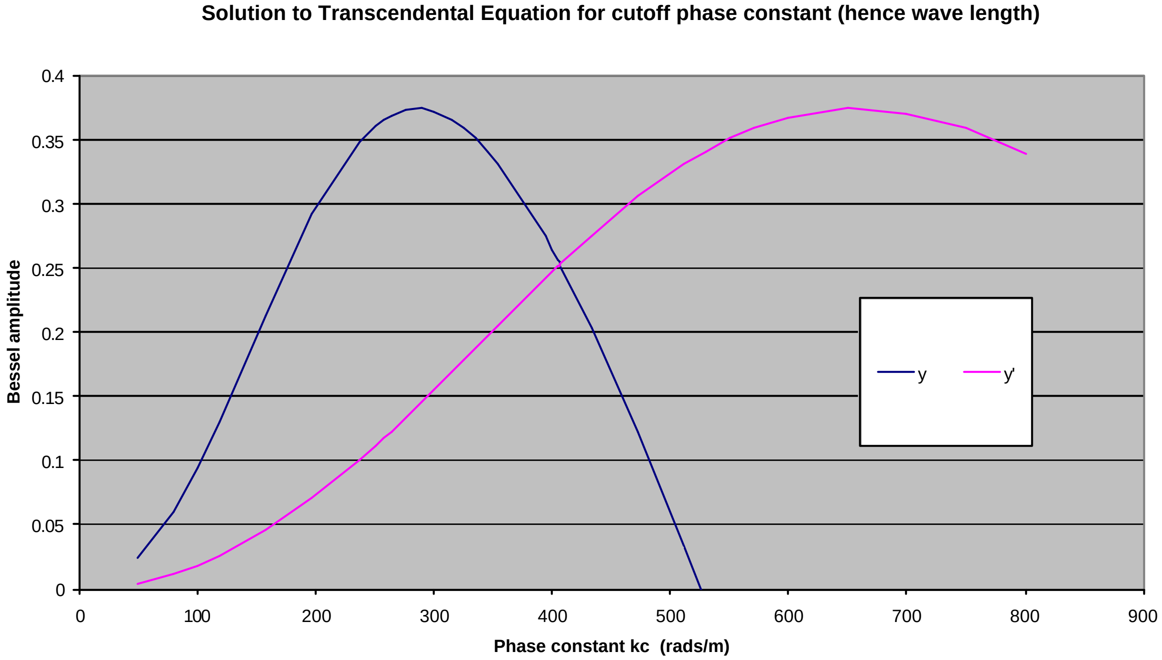

Figure 12 Solution to Transcendental Equation for cutoff phase constant (hence wave length)

B.2.1 Solving for TE_{12}

The preceding, of course, is for TE_{11}. That is the subscripts, (1), of Equation 28 and the first intercept in Figure 3.

If the x-axis is expanded the next intercept will relate to TE_{12}, then TE_{13} and so on as shown in Figure 13 below.

Here the first intercept can be seen at approximately 406 (TE_{11}) on the x axis, whilst the second occurs at approximately 1680 (TE_{12}) and the third at 3230 (TE_{13}).

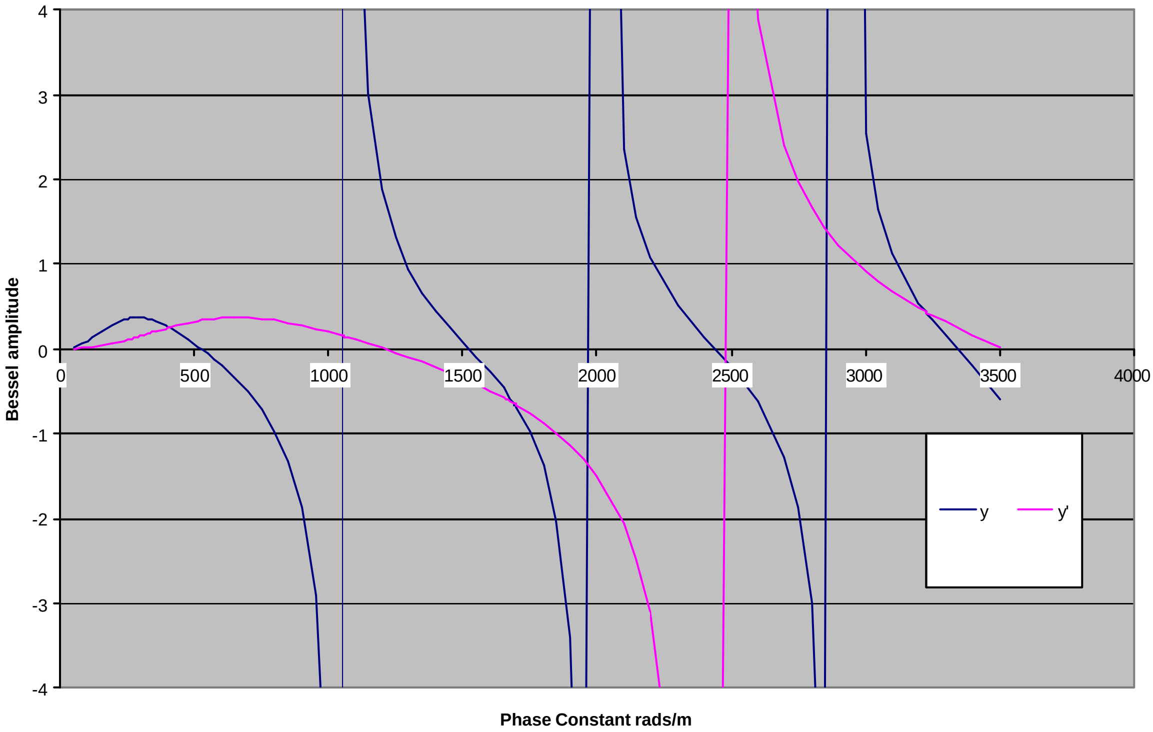

Figure 13 Solution to Transcendental Equation for cutoff phase constant. X-axis expanded to show TE_{12} and TE_{13}.

B.2.2 Solving for TE_{21}

In Equation 28, $J_1^{'}$ is the derivative of a Bessel function of the first kind *of order n = 1(mathematicians use v in place of n more often than not).* Similarly, $N_1^{'}$ is the derivative of a Neumann function or Bessel function of the second kind *of order n = 1.*

To obtain TE_{21} it is necessary to change the components of Equation 28 *to the order n =2.*

$$\frac{J_2^{'}(k_c a)}{N_2^{'}(k_c a)} = \frac{J_2^{'}(k_c b)}{N_2^{'}(k_c b)}$$

Equation 32

Again using the recurrence relations, ref.[9], a non-derivative form of Equation 31 may be derived:

Evaluating Equation 29 where $v = 2$ yields $J_2^{'} = J_1(x) - \frac{2x}{x^2} J_2(x)$

Equation 33

this result can then be substituted in Equation 32 and evaluated in a spreadsheet as before:

$$\frac{J_1(k_c a) - \frac{2(k_c a)}{(k_c a)^2} J_2(k_c a)}{N_1(k_c a) - \frac{2(k_c a)}{(k_c a)^2} N_2(k_c a)} = \frac{J_1(k_c b) - \frac{2(k_c b)}{(k_c b)^2} J_2(k_c b)}{N_1(k_c b) - \frac{2(k_c b)}{(k_c b)} N_2\ (k_c b)}$$

Equation 34

This expression is made up of functions of order $v = 1$ and $v = 2$ which the excel 'Function Wizard' will handle. However, traditionally, tables of Bessel functions, were only precise (adequate resolution) for J_0 and J_1. To this end the 'recurrence relations' ref.[8] can be employed resolve Equation 33 into components of J_0 , J_1, N_0 and N_1 as given below.

$$J_2^{'} = \left(1 - \frac{4}{x^2}\right) J_1(x) + \frac{2}{x} J_0(x)$$

Equation 35

Which when substituted in Equation 33 results in a slightly more complicated expression than that of Equation 34.

As in section B.2, a spreadsheet can be set up to locate the first intercept (TE_{21}), second (TE_{22}) , third (TE_{23}) and so on.

B.2.3 Solving for TE_{31}

Similarly, for TE_{31}, the above technique can be extended with the order $n = 3$ in Equation 32.

C Characteristic Impedance of TEM, TM and TE modes in coaxial line

C.1 Background

Elliott, ref.[6] puts forward a proposal to define Characteristic impedance for TEM, TM and TE modes where although the amplitude may be arbitrary the dependence on frequency, dimensions and material parameters is not.

It is considered important in the particular case, of this present report, that there is consistency when comparing the impedance presented to TEM and to TE waves on the same coaxial line. This implies that both definitions of Characteristic impedance should be dependent on the geometry and the material of the line.

Briefly, ref.[6] states that the transverse electric and magnetic fields for **any mode** propagating in the positive direction *z* along any rectilinear guiding structure, can be expressed in the form given in section 2.3 (main body report) then goes on to enlarge the relationship, for any mode (TEM, TM, or TE), propagating in the +*z* direction on any guiding structure, so as to define a mode voltage V(*z,t*) and a mode current I(*z,t*) by the equations:

$$\mathbf{E}_t(u,v,z,t) = K\mathbf{e}(u,v)e^{jwt-gz} = c_1 V(z,t)\mathbf{e}(u,v)$$

Equation 36

$$\mathbf{H}_t(u,v,z,t) = K\mathbf{h}(u,v)e^{jwt-gz} = c_2\, I(z,t)\mathbf{e}(u,v)$$

Equation 37

C.2 Characteristic Impedance of TEM mode on Coaxial Line

This eventually leads to the characteristic impedance, defined by Equation 14 for a TEM mode, now becoming generally applicable to all three mode types but in extended form:

$$Z_0 = \frac{V(z,t)}{I(z,t)} = \frac{V_0}{I_0} = \frac{K/c_1}{K/c_2} = \frac{c_2}{c_1}$$

Equation 38

To this point, the values selected for c_1 and c_2 are completely arbitrary. However there is a constraint on c_1 and c_2 involving the representation of instantaneous power flow. Using Equation 36 and Equation 37:

$$P = \int_S E_t \times H_t .dS = c_1 c_2 VI \int_S e \times h.dS$$

Equation 39

given that complex power flow is P=VI then:

$$\frac{1}{c_1 c_2} = \int_S e \times h.dS$$

Equation 40

For brevity, suffice it to say that the above can be developed to:

$$\frac{1}{c_1 c_2} = \frac{1}{Z_F} \int_S |e(u,v)|^2 dS$$

Equation 41

and that the constrained expression for the characteristic impedance is:

$$Z_0 = \frac{Z_F}{c_1^2 \int_S |e(u,v)|^2 dS} = \frac{c_2^2}{Z_F} \int_S |e(u,v)|^2 dS$$

Equation 42

Where Z_F is the field or wave impedance of the mode, that is Z_{TEM}, Z_{TM} or Z_{TE} as given in the main report at section 2.5.1. The value Z_0 assumes is still subject to the choice of c_1 or c_2 but not both.

*The important point is that Equation 42 defines Z_0 as a function of c_1 **or** c_2 and that c_1 can be evaluated where there is a transverse magnetic field (TM or TEM) and c_2 solved for the transverse electric field case (TE or TEM).*

C.3 Characteristic Impedance of TEM and TM mode on Coaxial Line

For TEM and TM modes ($H_z = 0$), if P_1 and P_2 are any two arbitrary points in S, the potential rise will be $-\int_{P_1}^{P_2} E_t.dl$ which can be identified as the mode voltage Z(*z*,*t*). This leads to:

$$\frac{1}{c_1} = -\int_{P_1}^{P_2} e(u,v).dl$$

Equation 43

after which, for TEM or TM modes, Equation 47 becomes:

$$Z_0 = Z_F \frac{\left[\int_{P_1}^{P_2} e(u,v).dl\right]^2}{\int_S |e(u,v)|^2 dS}$$

Equation 44

C.4 Characteristic Impedance of TEM and TE mode on Coaxial Line

Alternatively, for TEM or TE modes ($E_z = 0$), if C is any closed contour then $\oint_C H_t.dl$ equals the current enclosed. This can be defined as the mode current I(z,t), which leads to:

$$\frac{1}{c_2} = \oint_C h(u,v).dl$$

Equation 45

as a consequence, for TEM or TE, Eq C12 becomes:

$$Z_0 = \frac{1}{Z_F} \frac{\int_S |e(u,v)|^2 dS}{\left[\oint_C h(u,v).dl\right]^2}$$

Equation 46

The reference gives examples of the characteristic impedance for TEM mode calculated from both equations (C9 and 11) but not for a TE mode. This is given below:

C.5 Characteristic Impedance of TE mode on Coaxial Line.

Firstly the transverse co-ordinates (u,v) become (r,f), radius and angle, in cylindrical format. It is also necessary to appreciate that it can be shown that:

$$e = \frac{V_o}{\ln\left(\frac{b}{a}\right)} \frac{\hat{r}}{r} \quad and \quad h = \frac{\left(\frac{V_0}{Z_{TE}}\right)}{\ln\left(\frac{b}{a}\right)} \frac{f}{r}$$

where; Z_{TE} is given by equation 12 and V_0 is the potential rise from r = a to r = b.

From Equation 46:

$$Z_0 = \frac{1}{Z_{TE}} \frac{\left(\frac{-V_0}{\ln(b/a)}\right)^2 \int_a^b \int_0^{2p} \frac{dr}{r} df}{\left[\oint_C \frac{-V_0/Z_{TE}}{\ln(b/a)} . (\hat{r}\, dr + f df)\right]^2}$$

Equation 47

$$Z_0 = \frac{1}{Z_{TE}} \frac{\left(\frac{-V_0}{\ln(b/a)}\right)^2 . \ln(b/a). 2p}{\left[\frac{-V_0/Z_{TE}}{\ln(b/a)} \int_0^{2p} df\right]^2}$$

Equation 48

$$Z_0 = \frac{1}{Z_{TE}} \frac{\left(\frac{-V_0}{\ln(b/a)}\right)^2 . \ln(b/a). 2p}{\left[\frac{-V_0/Z_{TE}}{\ln(b/a)} \; .2p\right]^2}$$

Equation 49

$$Z_0 = \frac{1}{Z_{TE}} (Z_{TE})^2 . \frac{\ln(b/a)}{2p}$$

Equation 50

Recalling the wave or field impedance Z_{TE} from Equation 12 in the main body of the report, leads to the characteristic impedance of a TE mode on coaxial line as:

$$Z_0 = \frac{h}{\sqrt{e_r}} \frac{1}{2p} \ln\left(\frac{b}{a}\right) \frac{1}{\sqrt{1 - \left(\frac{l}{l_C}\right)^2}} \quad for \; l \leq l_C$$

Equation 51

or

$$Z_0 = j \frac{h}{\sqrt{e_r}} \frac{1}{2p} \ln\left(\frac{b}{a}\right) \frac{1}{\sqrt{\left(\frac{l}{l_C}\right)^2 - 1}} \quad for \; l \geq l_C$$

Equation 52

Initial distribution list

ASAP Calibration Services Ltd
Information Resources
Project File

External
Alistair Hooley, DTI NMS, London SW1W 9SS
10 copies

This page intentionally left blank